中國機械工程學刊第四十六卷第二期第 163~172 頁(民國一百一十四年)
Journal of the Chinese Society of Mechanical Engineers, Vol.46, No.2, pp 163~172 (2025)

Analysis and Optimization of Dynamic Characterization for Series-Parallel Shipboard Stabilized Platforms

Tian Zeng*, Hai-Feng Zhang**,Di-Qing Fan***, Xin-Tian Liu****
and Bo Tong*****

Keywords: tandem stabilization platform, system control, robustness, dynamic property

ABSTRACT

To address the problems of complex structure, high cost, and weak stability of the traditional shipboard stabilization platform, this work proposes a series-parallel shipboard stabilization platform, which consists of a series mechanism and a parallel mechanism composite and has the advantages of simple structure, good stability and high control accuracy. In this work, the platform's robustness was analyzed, and experiments on the control accuracy and dynamic characteristics were performed based on four operating states of the ship. The results show that the platform can effectively inhibit ship sway, has good dynamic characteristics and control accuracy, and can satisfy the application requirements of a miniaturized, low-cost, and highly dynamic shipboard stabilization platform.

INTRODUCTION

During a ship's voyage, due to the influence of sea surface wind and waves, there will be swaying and undulating motion, which seriously affects the information collection of shipborne equipment, such as the launch of shipborne laser weapons and container transportation of offshore cranes (Saghafi et al., 2021). The stabilization platform isolates the effects of multi-dimensional coupled perturbations on carrier stability through a set of online signal detection and real-time motion compensation mechanisms to control the stability of carriers attached to the ship. Marine operations require high safety and stability of the ship, and the stabilized platform, as key equipment, can effectively isolate the disturbance caused by the movement of the ship in complex marine environments and ensure the stable operation of the platform equipment.

In the complex marine environment, the role of shipboard stabilized platforms is mainly to compensate for the movement of their loads, and changes in heading and rocking of the ship will perturb the platform system (Hu et al., 2020; Hu et al., 2018; Luo et al., 2010; Yang et al., 2020) and the practice of a three-degree-of-freedom ship model with dynamic instability and perturbation (Zhang et al., 2022; Zhang et al., 2022; Zhang et al., 2019). In this case, the shipborne stable platform can automatically calibrate its pose through connecting shafts (Lin et al., 2023), reduce the influence of nonlinear vibrations on the axis (Wang et al., 2021), ensure the stability of the platform relative to the inertial coordinate system, and enable the carrier to accurately track the target during maritime motion. Many factors affect the stability of a ship, including whether cargo loading and unloading are appropriate, whether the main scale design of the ship is reasonable, waves on the deck, free liquid level, and other influencing factors; hence, the development of wave compensation technology is very important (Rong et al., 2019).

Currently, the international development of stabilization platforms mainly focuses on improving the accuracy, integration, signal processing and system control algorithms (Zhao et al., 2021). Extensive research has been conducted on stable platform control problems with uncertain model parameters and external disturbances. In the field of

Paper Received July, 2024. Revised September, 2024. Accepted October, 2024. Author for Correspondence: Hai-Feng Zhang.

** Graduate Student, School of Mechanical and Automotive Engineering, Shanghai University of Engineering Science, Shanghai 201620, China.*

*** Associate Professor, School of Mechanical and Automotive Engineering, Shanghai University of Engineering Science, Shanghai 201620, China.*

**** Senior engineer, School of Mechanical and Automotive Engineering, Shanghai University of Engineering Science, Shanghai 201620, China.*

***** Professor, School of Mechanical and Automotive Engineering, Shanghai University of Engineering Science, Shanghai 201620, China.*

****** Senior engineer, Department of R&D, Xi'an Thermal Power Research Institute Co., Ltd, Xi'an 710032, China.*

serial stable platform control, Qu et al. (2020) proposed an improved nonlinear active control strategy, Zhang et al. (2019) designed an adaptive hyper twisted sliding mode control scheme based on an extended state observer, and Wang et al. (2020) proposed a three-axis stable platform scheme using adaptive non-singular fast terminal sliding mode control. However, due to structural limitations, the load-bearing capacity of the series platform is limited, which makes it difficult to effectively compensate in the heave direction. This problem can be effectively solved in parallel platforms. Qiang et al. (2020) proposed a predictive control stability strategy for a parallel Stewart structure shipborne platform based on the ship motion prediction. Yuan et al. (2024) designed an electro-hydraulic driven 3-UPS/S parallel stable platform based on multi-axis coupled motion. The electro-hydraulic drive technology significantly improves the load-bearing capacity, stiffness, and control accuracy of the platform. Liu et al. (2022) also designed an adaptive hyper twisted sliding mode control law based on an extended state observer to stably control a three-axis parallel shipborne platform. However, due to the uncertainty of wave motion, series platforms are more stable than parallel mechanisms in compensating for external disturbances during nonlinear vibrations of the mechanism. Based on its stability and robustness (Cai et al., 2021), a three-degree-of-freedom series-parallel architecture of the stabilization platform was proposed, and the series-parallel platform has a high load, multi-axis coupled motion function (Zhao et al., 2016; Liu et al., 2019; Xu et al., 2017). Mazare et al. (2017) verified the rationality of the architecture based on the kinematic analysis of ADMAS.

In this study, a new series-parallel stabilized platform was designed with a new series-parallel joint drive and a new multi-sensor combined MEMS gyroscope as the position detection input. Based on the separated PID control algorithm, the stabilized output of the joint motor control was realized, the dynamic accuracy of the stabilized platform was verified by the software, and the dynamic accuracy of the stabilized platform was verified by the software and further analyzed via experimental data collection.

STABILIZED PLATFORM SYSTEM

During sailing, a ship is subject to four main types of motion: roll, pitch, yaw , and heave (Perez et al., 2019). As shown in Fig. 1, they include rotary motion around the X-axis (roll), rotary motion around the Y-axis (pitch), rotary motion around the Z-axis (yaw), and up and down motion along the Z-axis (heave). These four synthetic inertial forces are the main external forces, and the existence of external forces inevitably affects the movement of the cargo. The stabilization platform designed in this work mainly aims at the inertial forces in the four directions of the movement of the vessel for compensation to ensure the smoothness of the cargo.

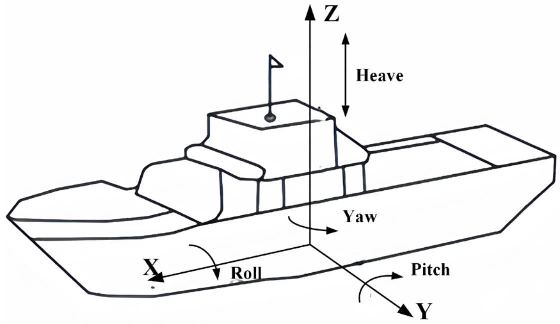

Fig. 1. Schematic diagram of the ship movement

Components of the Stabilization Platform

The composition of the shipboard stabilization platform system includes four major modules, as shown in Fig. 2. The control system is the core, the platform structure is the foundation, the drive power system is the key, and the scheme design of each module determines the overall performance of the entire system.

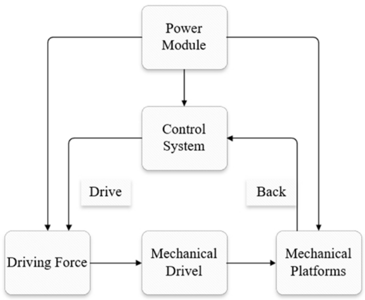

Fig. 2. Stabilized platform system components

At sea, under the influence of wind and waves, a ship will produce roll and pitch and other motions of a certain amplitude, which will cause serious interference with information acquisition and object data tracking and affect the normal function of the carrier. It is necessary to mitigate the impact of such interference using a stabilization platform. The stabilizing platform uses the reverse motion of the motor to eliminate the rocking motion of the ship to achieve a stable attitude of the ship carrier. This process involves the online attitude acquisition real-time control compensation and other high-precision control requirements. For different applications, the performance standard is different: the series-parallel stabilizing platform designed in this work is mainly applied to the small platform system of the ship, and the carrier carried is also smaller. In addition, the precision requirements are greater, and the four types of fluctuations affect the ship's non-stability put forward the parameter accuracy design requirements, as shown in Table 1.

The dynamic accuracy of the stabilized platform mainly considers the final accuracy required by the control error, transmission error, installation error, and sensor error. The pendulum direction error is compensated by the lifting and sinking mechanism, and its overall error is controlled at ±2 mm. The stabilized platform is special equipment, and the working environment is mostly outside the ship, which is in harsh conditions. Hence, many dynamic characteristics and requirements for the actuators and controllers of the platform are proposed.

Table 1. Parameter accuracy design requirements

Parameters	Pendulum	Cyclicality	Speed	Accurate
Roll	±16 °	4 s	60 rpm	±1 °
Pitch	±16 °	4 s	60 rpm	±1 °
Yaw	73 mm	2 s	120rpm	±2 mm
Heave	±90 °	6 s	10 rpm	±1 °

Due to the uncertainty of the real-time steady state of the stabilized platform and high load requirements, at this stage, to improve the excellent characteristics of the platform, the series-parallel hybrid stabilized platform mechanism can be used. The use of a series-parallel hybrid can effectively improve the design conditions of the engine, so that the engine is in the optimal operating state, and the parallel mechanism of the series-parallel shipboard stabilized platform can be constructed using the self-imposed perturbation control technology. The expansion of the state observer and parallel mechanism of the tandem-parallel shipboard stabilization platform can use the self-anti-turbulence control technique to construct an expansion state observer, which estimates the total perturbation in real time. The total perturbation consists of the dynamic uncertainty of the shipboard stabilization platform, the unknown time-varying external perturbation, and the coupling among various degree-of-freedom motion state variables of the platform to realize the stabilization control of the platform.

Design of Series-Parallel Stabilized Platforms

Considering the platform's performance requirements, such as light load, compact size, and rapid response, employing only parallel connections would undoubtedly lower the dimensionality of the motion space and compromise flexibility, potentially failing to satisfy the platform's specifications. After comprehensive consideration, the platform uses a series–parallel hybrid connection form with its overall structural diagram in Figure 3. The series-parallel mechanism was first proposed by Waldron et al. (1989), which combines the advantages of series and parallel mechanisms and consists of a 3-degree-of-freedom series module and a 7-degree-of-freedom parallel module (Tang et al., 2019). This three-degree-of-freedom stabilized platform can compensate for more than 98% of wave-induced ship movement (Ya et al., 2023; Liu et al., 2023). The PID method enables a series-parallel stabilized platform to compensate for the roll and pitch angles of the unmanned vessel and the pendulum motion of the vessel by controlling the coordinated rotation of the three struts (Niu et al., 2022).

Figure 4 shows a schematic diagram of the parallel mechanism on the upper half of the stable platform. The components are connected by motion pairs. Assuming that the constraint force caused by the i-th motion pair is u_i, the number of motion pairs is g, the total number of components is n, and the total degree of freedom M is

$$M = 6(n-1) - \sum_{i=1}^{g} u_i \tag{1}$$

As illustrated in Figure 4, the schematic diagram of the parallel mechanism on the upper half of the stable platform shows 6 rotating pairs and 3 spherical pairs. Each rotating pair has 1 degree of freedom, whereas each spherical pair has 3 degrees of freedom. With a total of n=8 components, the system has a calculated degree of freedom of 3.

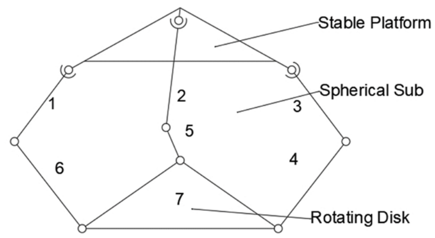

Fig. 3. Stabilization platform structure sketch

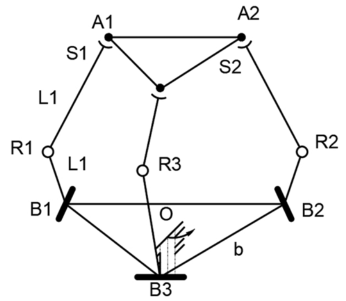

Fig. 4. Sketch of series–parallel connections

The mechanism design, as shown in Fig. 4, consists of a stabilizing platform surface (upper platform), a lower platform surface, and three *RRS* chains of the same structure. The stabilizing platform surface *A1A2A3* is connected to the rods through the spherical vice (*S*), the lower platform surface *B1B2B3* is connected to the rods through the rotating vice (*R*), the two rods are connected by the same rotating vice (*R*), and the base surface *B1B2B3* has a stepping motor at its center point *O*, which is connected to the base surface through the rotating vice (R). The base surface *B1B2B3* is connected to the base surface at its center point *O*. Stepping motors are provided at points *B1*, *B2,* and *B3* to control the swinging motion of the support chain, and a rotary motor is connected in series at point *O* to realize the overall rotary motion. The lower shaft L1 and the upper shaft *L2* are 150 mm long, and the equilateral triangle *b* of the stabilized platform surface is 260 mm long. *L1* and *L2* are 150 mm, and length *b* of the equilateral triangle on the stabilized platform is 260 mm. *C* and β represent the lower end of the shaft, the upper end of the shaft, and the horizontal position of the angle from the axis to the angle. The minimum value of *C* and the minimum value of β are 135° and 125°, respectively, and the maximum values of *C* and β and the maximum values of β are 55° and 145°, respectively. The d_h and d_l represent the highest and lowest values of the pendulum motion range, which are calculated by Eq. (1) and Eq. (2), respectively:

$$d_h = L_1 \cdot \sin(\alpha_{\max}) + L_2 \cdot \sin(180 - \beta_{\min}) \tag{2}$$

$$d_l = L_1 \cdot \sin(\alpha_{\min}) + L_2 \cdot \sin(180 - \beta_{\max}) \tag{3}$$

where the roll and pitch angles θ are calculated using Equation (4):

$$\theta = \arcsin\left(\frac{d_h - d_l}{b \cdot \sin\pi / 3}\right) \tag{4}$$

Table 2. Parameter design of the stabilizing platform

	Upper shaft1	Upper shaft2	Upper shaft3	Lower shaft1	Lower shaft2	Lower shaft1
Shaft length(mm)	$L_1 = 150$			$L_1 = 150$		
Shaft angle (°)	$\alpha(35 \sim 55)$			$\beta(125 \sim 145)$		
Swing range (mm)	$d = (d_l \sim d_h) = (172 \sim 245)$					
Swing angle (°)	$\theta = \pm 16$					

The specific parameters of the stabilizing platform mechanism design are shown in Table 2. The limit range to compensate for the horizontal and vertical rocking angles is 16°, and the limit range for the pendulum motion is 73 mm. In addition, a single rotary stepping motor is set up in the base chassis, and the rotation of the platform is independently controlled by this motor to maximize the rotation angle.

The series parallel stable platform of the system is composed of articulated linkage actuators. As illustrated in Fig. 5, the platform body comprises a stable platform surface, a chassis, and three sets of articulated rods. The articulated rods are connected to the stable platform surface through universal joints and form an equilateral triangular structure. The platform is used to install stable equipment and detect tilt angles through attitude measurement devices. The stabilizing mechanism includes universal joint, upper shaft end, lower shaft end, and rotating vise driven by an electric motor to ensure that the platform remains stable during the ship's roll and pitch. The control system drives the motor to adjust the posture based on the information from the posture sensor.

The platform surface has positioning holes that can be used to install fixtures to fix the load. The MEMS gyroscope is used to sense the tilt and attitude deviation of the platform and ensure stability through real-time adjustment. The platform base is a three-chain parallel mechanism, with motors distributed in an equilateral triangle to drive the rotation of parallel branch chains, thereby maintaining the stability of the platform. The lower platform is equipped with a reducer and a rotating motor, which are fixedly connected to the hull to maintain the consistency of platform movement.

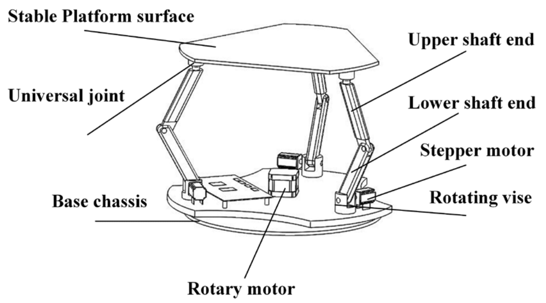

Fig. 5. Structural schematic

Control Design

The inertial measurement unit transmits the detected values to the control center, which performs the attitude calculation and data transmission. Then, the control center calculates the error value between attitude sensor and coordinate system and sends the error value to the PID control submodule. The PID control submodule processes the error value and outputs a pulse width modulation PWM control signal from the control motherboard, which is transmitted to the motor drive unit through the external output circuit of the motor. Finally, the stepper motor is driven to rotate a predetermined angle to adjust the platform posture.

A finite element analysis was conducted on key components, including the upper shaft, lower shaft, motor support seat, and cross universal joint, employing the overall force distribution method with a set load force of 1000N. The maximum deformation of the upper shaft cross universal joint and lower shaft motor seat was 0.0288 mm, 0.0200 mm, 0.0417 mm, and 0.0460 mm, respectively. The maximum stress measured on the motor base was 21.06 MPa, while the yield stress of the Al plate used was 90 MPa. These results indicate that the component can satisfy practical requirements within its safety factor of 4.27.

To improve the performance of PID control and make the motor run more smoothly, the PID was improved and perfected. Improved PID control is based on the PID algorithm and adopts the integral separation algorithm.

While $|\ e(k)| > \varepsilon$, use PD control below:

$$u(kT) = K_P e(kT) + K_D[e(kT) - e(kT - T)] \tag{5}$$

While $|\ e(k)| \le \varepsilon$, use PID control below:

$$u(kT) = K_P e(kT) + K_E K_I \sum_{j=1}^{k} e(jT) + K_D[e(kT) - e(kT - T)] \tag{6}$$

The control upper computer interface is shown in Figure 6.

Fig. 6. Physical diagram of the stabilizing platform

STABILITY AND ROBUSTNESS

Stability analysis and robustness analysis of ships are important parts of ship design and operation to ensure the safe operation of ships under various conditions. Stability analysis focuses on the behavior of a ship in the absence of external perturbations, whereas robustness analysis focuses on the performance of a ship in the face of external perturbations.

Stabilize Platform Stability

Ship stability refers to the case that when a ship under the action of an external moment deviates from its initial equilibrium position and tilts, the ship can resist the external force and restore the original equilibrium state when the external moment is eliminated. The ship stability is important for ensuring ship safety. Here, the experimental level is simulated by adding the corresponding load, and the upper computer collects the angle data of the movement process through the MEMS gyro.

Fig. 7. Experimental acquisition diagram

To test the dynamic accuracy of the platform, after the system had been powered on, the program was downloaded, and the initial state was set to 0°. The platform acted in concert with the three chains, and chain A was set to the X-axis to move to a horizontal swing angle of 15°. The host computer collected the angle data of the movement process through the MEMS-stabilized gyro, and the actual data collection used video recording. When measuring the roll angle, the inclination data of the stabilized platform under dynamic conditions are collected by the goniometer; when performing the vertical swing height measurement, the laser pointer-assisted method is used to read the height data on the scale. The current goniometer reading was collected every 0.1 s, and the curve was plotted. Figure 7 shows the experimental acquisition diagram.

Figure 8 illustrates the relationship between the roll angle and the gyroscope compensation output angle. During the rotation of the platform device, the difference between collected roll angle data and gyro output angle is large in the starting state. With time, the device self-adjusts, and the roll angle data coincide with the data measured by the upper computer. The main reason for the large difference is that the platform angle is adjusted by the short PWM pulse received by the motor, the torque on the motor in the starting state is large, and there is a mutual interference among the three chains. This interference stabilizes the platform action, so that the motor suddenly accelerates to the highest speed and subsequently quickly reduces to zero, which generates a large impact in the process, causes impact and vibration on the motor, coupling, shaft connection, etc., and leads to an inertial unit and measurement of zero. Vibration results in inertia unit and goniometer readings and produces small changes, which indicates that the phenomenon of the curve in the figure partially does not overlap. Later, the curves coincide because the device has the functions of self-regulation and self-compensation. In Fig. 8, the two curves of the inclination angle of roll and the output angle of gyroscope compensation coincide, which can verify that the stabilized platform has good compensation for roll to maintain balance, and the platform has stability.

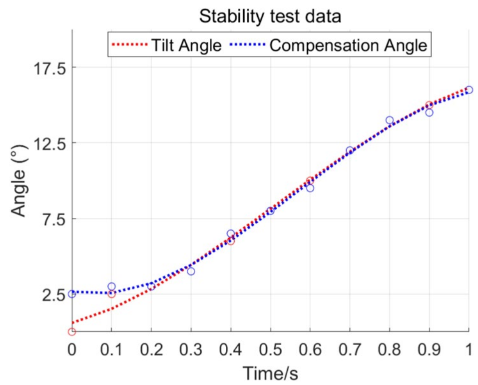

Fig. 8. Stability test data

Stabilizing Platform Robustness

Robustness analysis of a ship refers to the robustness of a ship's stability analysis method to ensure the reliability of the analysis results. To be precise, robustness analysis aims at the ability of the ship's stabilization platform to remain relatively robust under conditions of external disturbances.

When the carrier on the ship is disturbed by different factors such as wind, waves, and collisions, there will be a sudden rise or fall in different directions. At this time, the stabilized platform can use the reverse movement of the motor to compensate for the carrier's movement and maintain its movement stability. An example of the pendulum motion is as follows: when the carrier is disturbed by external wind, waves and other unstable factors, there is a sudden rise in direction of gravity, as shown in Figure 9(a); at this time, the stabilized platform on the surface of the carrier also tends to move upwards. The stabilized platform drives the lower-end axis to move clockwise or the upper-end axis to move counterclockwise through the motor, which makes the platform descend, as shown in Fig. 9(b), to compensate for the pendulum movement in the direction of gravity and to keep the carriers installed on the stabilized platform in a stable attitude.

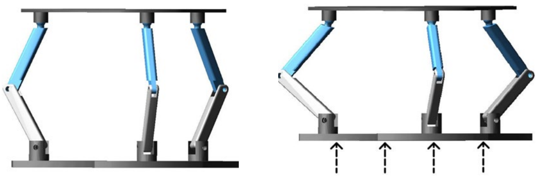

(a) Before SPC (b) After SPC

Fig. 9. Stabilized platform compensation (SPC)

Since the previous stability platform dynamic accuracy analysis is different, the robustness analysis here aims to add an ocean wave simulation experiment. This study shows that the ocean wave curve is a multi-level sinusoidal function. To make the disturbance input function closer to the wave curve and reflect the effect of the experiment, the rotational perturbation function was set as a sinusoidal function *sint* to obtain the roll fluctuation $a = (sint)/4$ and pitch fluctuation $b = (cost)/4$. According to the kinematics analysis model, the altitude was solved using MATLAB, and the solving data were imported into the ADAMS model to perform the dynamic simulation.

The stabilized platform was installed and commissioned for actual dynamic analysis. To obtain more obvious comparison data, the input dynamics were tested separately for roll and pitch compensation, and the stabilized platform surface was set to be in a sinusoidal fluctuation perturbation environment. The angle information was collected by the inertial measurement unit and compared with the actual running function. The actual dynamic test data were collected by the camera device, and the actual motion displacement of the stabilized platform was plotted. The information collected by the inertial measurement unit was analyzed, and the error was compared with the change curve of the center of mass of the platform surface to verify the error compensation performance of the platform.

The information collected by the inertial measurement unit was analyzed and compared with the change curve of the center of mass of the platform surface to verify the error compensation performance of the platform, as shown in Figure 10.

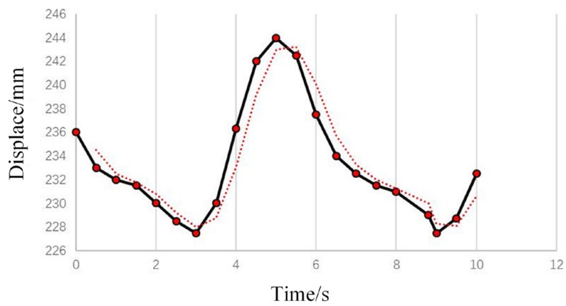

Fig. 10. Comparison of the displacement trajectories

The red dashed line represents the curve of the platform position change, and the black solid line represents the data collected by the inertial measurement unit of the upper computer. Notably, the curve does not completely overlap with the image in the absolute environment, and its maximum tracking error is approximately 1.7 mm, which satisfies the parameter requirements. Its subsequent error is mainly due to the platform in actual operation and the gap caused by the mechanism, including the installation gap, transmission gap, bearing gap, and shaft hole fit gap. The size of these gaps has a relatively large effect on the accuracy.

Experimental Test

To test the stability accuracy of the platform, after the system had been turned on, the program was imported. According to the previous operational analysis and calculation of the motor rotation angle relationship, the instruction was input to control the motor to rotate at a certain angle so that the platform roll angle stabilized at 0 °, 5 °, 10 °, 15 °, and these values were compared and analyzed with the actual angle measured by the goniometer. To test the roll performance of the motor, load performance test experiments were conducted for 0.0 kg, 0.5 kg, 1 kg, and 2 kg for data acquisition. Multiple measurements were performed, and the average value was obtained. The results of the rolling experiment are shown in Table 3, and the experimental data were processed and calculated to obtain the motion error of the roll experiment, as shown in Fig. 11. The experimental performance was analyzed by comparing the set parameters.

Experimental analysis of the roll: the rated load of the platform was 0.5 kg; the movement positioning error under this load was approximately 0.55°; the movement positioning error under 1-kg load was 0.95°; the positioning error under 2-kg load was more than 1.85°; according to the requirement of the platform performance setting parameter, the roll error was <1°, and the platform was invalidated under this load.

Table 3. Results of the roll experiments

Serial number	Experimental Projects	Experimental data (°) 0 °	5 °	10 °	15 °
1	Roll (unloaded)	0	5.13	10.35	14.78
2	Roll (0.5 kg)	0	4.85	9.72	14.45
3	Roll (1 kg)	0	4.71	9.60	14.05
4	Roll (2 kg)	0	4.26	9. 12	13.15

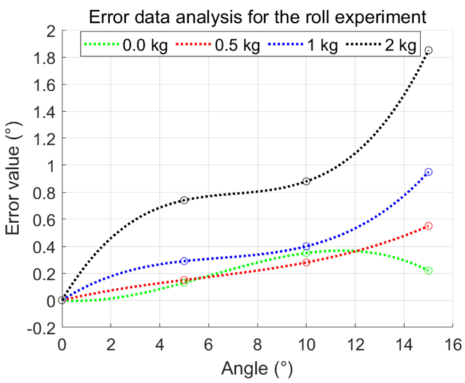

Fig. 11. Error data analysis for the roll experiment

Table 4. Results of the pitch experiments

Serial number	Experimental Projects	Experimental data (°) 0 °	5 °	10 °	15 °
1	Pitch (unloaded)	0	5.11	10.20	15.28
2	Pitch (0.5 kg)	0	4.83	9.61	14.38
3	Pitch (1 kg)	0	4.68	9.56	14.09
4	Pitch (2 kg)	0	4. 12	9.03	13.25

For the pitch test, the pitch angle was 0°, 5°, 10°, or 15°, and the actual angle was measured by a goniometer for the comparison experiments. Similar to the roll test, the unloaded state and loads of 0.5 kg, 1 kg, and 2 kg were used for data collection, and multiple measurements were taken to obtain the average values. Experimental results are shown in Table 4, and the experimental data were processed and calculated to obtain the motion error of the pitch test, as shown in Figure 12.

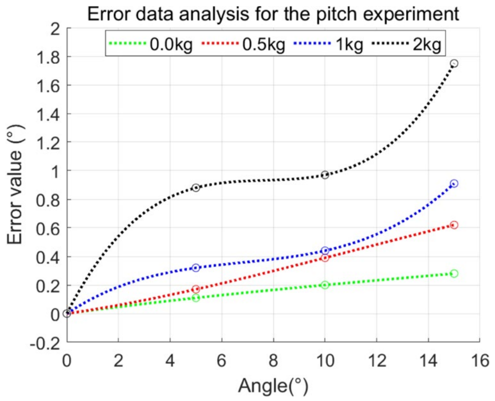

Fig. 12. Error data analysis for the pitch experiment

Experimental analysis of the pitch: The platform has a rated load of 0.5 kg, the movement positioning error was approximately 0.62°, the load was 1 kg, the movement positioning error was 0.91°, the load was 2 kg, and the error exceeded 1.75 °, which indicates the basic failure.

Table 5. Results of the yaw experiments

Serial number	Experimental Projects	Experimental data (°) 0 °	30 °	60 °	90 °
1	Yaw (unloaded)	0	30.45	60.25	89.82
2	Yaw (0.5 kg)	0	30.25	59.85	90.28
3	Yaw (1 kg)	0	30.28	60.02	89.63
4	Yaw (2 kg)	0	30.25	59.35	89.48

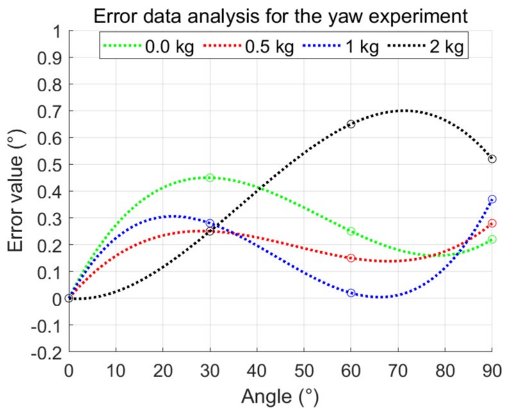

Fig. 13. Error data analysis for the yaw experiment

The ship is less disturbed by the yaw direction during sailing, so the yaw rotation motor was used as an active compensation motor; i.e., when the stabilizing platform rotates at a large angle, the upper computer can give commands to adjust the stabilizing platform to the specified state. The rotation angle measurements were made at 0°, 30°, 60° and 90°, and experimental data were collected for no load and various types of analog loads. The motion errors of the yaw experiment are shown in Table 5, and the experimental errors are analyzed in Figure 13.

Experimental analysis of the yaw: Since the yaw motor carries the overall weight of the platform device, the selected motor performed better than the articulated stepping motor. From the experimental data, the error range of the selected motor was <1 ° under the simulated load of 3 kg, which satisfies the requirements of the setup index.

Heave is a coordinated motion of three chains with the same speed in the direction of motor rotation, which is theoretically smaller than the error range of the roll and pitch angles and yaw angles. The experimental swing distances were set to 10 mm, 20 mm, 40 mm, and 60 mm, and the data were collected under no load, 0.5 kg, 1 kg, and 2 kg, respectively. The Heave experimental results are shown in Table 6, and a motion error analysis of the heave experiment was performed, as shown in Fig. 14.

Table 6. Results of the heave experiments

Serial number	Experimental Projects	Experimental data (mm) 10	20	40	60
1	Heave (unloaded)	10.08	20.04	40. 12	57.60
2	Heave (0.5 kg)	9.89	19.86	40.03	58.70
3	Heave (1 kg)	9.82	19.81	39.85	58.10
4	Heave (2 kg)	9.72	16.50	36.37	54. 12

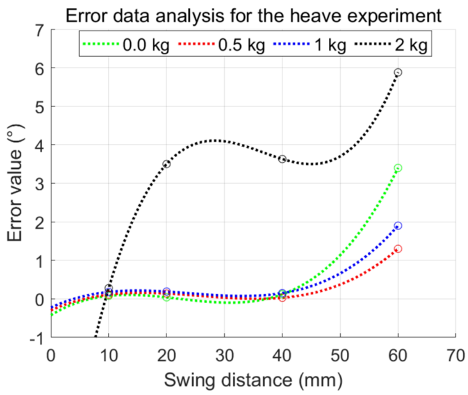

Fig. 14. Error data analysis for the heave experiment

The rated load of the platform was set to 0.5 kg, the error of motion positioning under this load was approximately 0.14 mm, the error of motion positioning under the load of 1 kg was 0.19 mm, and the error under the load of 2 kg was more than 5.88 mm, which is ineffective at this time. Thus, there is a limitation of the load under the simulation, and the loading and unloading of large cargoes are important factors to stabilize onboard platforms during their use. Therefore, we must adjust the shipboard stabilized platform to satisfy the dynamic characteristics of a large weight load.

Stable Platform Dynamic Characteristics Optimization

After the experimental test of the stabilized platform, the accuracy of the parameters of the load at 1 kg and below is designed in the range of requirements. In the case of 2 kg, the roll, pitch, yaw and heave might satisfy the requirements and dynamic characteristics of the shipboard stabilized platform of the large-weight load, and they must be readjusted. In actual mechanical applications, mechanical and control factors affect the accuracy of the platform, and the structural layout of the mechanical transmission equipment has an important effect on the accuracy of the transmission. A reasonable structural layout simplifies the structure, increases the overall strength and reduces the transmission error.

Adjustments to the Stabilization Platform

In this work, the motor shaft in the stabilization platform is driven by the rotating lower-end shaft through rigid coupling, which is a rigid transmission with large damping and unstable transmission. The rigid coupling structure is simple and does not compensate for axial displacement or radial displacement. Optimizing the loading damping structure and flexible transmission mode can further reduce the error, improve the smoothness of the transmission process, reduce transmission noise, and improve the transmission accuracy. Here, the original rigid coupling is replaced with flexible coupling with a diaphragm as the connection of the motor-driven lower-end shaft drive, which can maintain high synchronization with the brake while satisfying the compensation of shaft end deviation. We select the XD6-C26 coupling with a smaller deviation as the connection of the motor-driven lower shaft drive.

After the rearrangement, the reducer was connected to the lower platform surface via coupling, as shown in Figure 15.

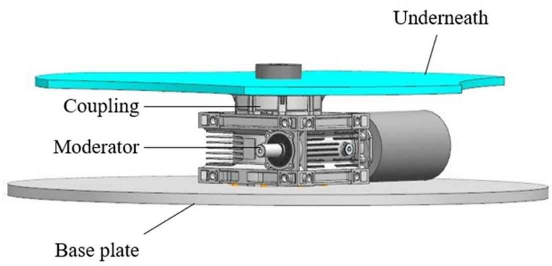

Fig. 15. Optimized structure of the rotating device

Data Analysis

To construct the experimental platform, we turned on the stabilization platform and conducted experiments to obtain the results of the insight experiments under four modes (roll, pitch, yaw, heave) and a load of 2 kg. Fig. 16 compares the results before and after optimization.

According to the ship stabilized platform accuracy design requirements, the initial design of the stabilized platform and optimized test results were compared. Finally, the measurement error between these two platforms was calculated, as shown in Fig. 16. The error of the stabilized platform decreased after optimization, the errors of rolling, pitching and yawing were less than 1°, the error of heaving was less than 2 mm, and the measurement accuracy satisfy the requirements.

Based on the above analysis, the proposed series-parallel stabilized platform for ships can solve the disturbance problem when sailing, and the optimized platform can satisfy the requirements even under large loads in terms of anti-interference. The series-parallel stabilized platform is simpler in structure, more targeted, and has a wider application range than the traditional six-degree-of-freedom platform.

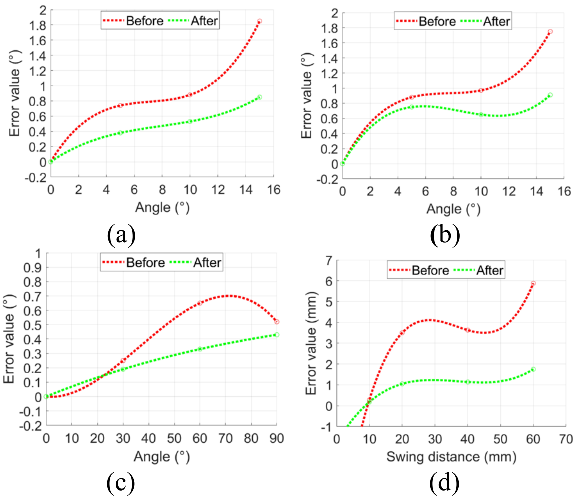

Fig. 16. Comparison plots before and after optimization; (a) roll; (b) pitch; (c) yaw; (d) heave

CONCLUSIONS

In this study, a novel series parallel stable platform system was proposed, which achieved precise compensation for ship's roll, pitch, yaw, and heave. The reliability and stability of this system were verified through simulation and experimental verification, and the structure is simple and feasible. The highlights of this work are as follows:

(1) The platform adopts three sets of branch parallel mechanisms and series rotating mechanisms and the integral separation PID algorithm to achieve stable output of the system.

(2) Reliability analysis and experimental verification have confirmed that the system can compensate for pose errors caused by the roll, yaw, pitch, and heave.

(3) Although the roll yaw angle error of the system design is 1 degree and the heave distance is 2 mm, the error accuracy can be improved by optimizing the damping coefficient and stiffness coefficient.

(4) This series parallel stable platform system has the advantages of simple structure and good universality and can be used for military operations and industrial applications on ships.

In summary, the proposed series parallel stable platform system in this article is simple and feasible and can improve the accuracy of ship pose compensation for stable platforms under external disturbances of wave uncertainty.

ACKNOWLEDGMENT

The authors acknowledge the contributions of all co-signers to this manuscript. This work is supported by the Class III Peak Discipline of Shanghai—Materials Science and Engineering (High-Energy Beam Intelligent Processing and Green Manufacturing).

REFERENCES

Cai, Y.F., et al. "Adaptive robust dual-loop control scheme of ship-mounted Stewart platforms for wave compensation." *Mechanism and Machine Theory* 164 (2021): 104406.

Hu, X, et al. "Asymptotic regulation of dynamically positioned vessels with unknown dynamics and external disturbances." *The Journal of Navigatio* 73.2 (2020): 253-266.

Hu, X, et al. "Robust adaptive NN control of dynamically positioned vessels under input constraints." *Neurocomputing* 318 (2018): 201-212.

Lin, C.J., H.C. Wang, and C.C. Wang. "Automatic calibration of tool center point for six degree of freedom robot." *Actuators*. Vol. 12. No. 3. MDPI, 2023.

Liu, W.J., et al. "Stabilization control of 3-DOF parallel vessel-borne platform with dynamic uncertainties and unknown disturbances." *Applied Ocean Research* 126 (2022): 103271.

Liu, Z.L., J Wu, and D Wang. "An engineering-oriented motion accuracy fluctuation suppression method of a hybrid spray-painting robot considering dynamics." *Mechanism and Machine Theory* 131 (2019): 62-74.

Luo, E, et al. "A 3-DOF coupling parallel mechanism for the stabilized platform and its motion characteristics." *Jiqiren(Robot)* 32.5 (2010).

Mazare M, Mostafa T, and M. Rasool N. "Kinematic analysis and design of a 3-DOF translational parallel robot." *International Journal of Automation and Computing* 14 (2017): 432-441.

Niu, A.Q., et al. "Dynamic modeling and analysis of a novel offshore gangway with 3UPU/UP-RRP

series-parallel hybrid structure." *Ocean Engineering* 266 (2022): 113122.
Rong, B, et al. "Dynamics analysis and wave compensation control design of ship's seaborne supply by discrete time transfer matrix method of the multibody system." *Mechanical Systems and Signal Processing* 128 (2019): 50-68.
Qiang, H.B., et al. "Model predictive control of a shipborne hydraulic parallel stabilized platform based on ship motion prediction." *IEEE Access* 8 (2020): 181880-181892.
Qu, J.J., et al. "Modified ADRC for inertial stabilized platform with corrected disturbance compensation and improved speed observer." *IEEE Access* 8 (2020): 157703-157716.
Waldron, K.J., M. Raghavan, and B. Roth. "Kinematics of a hybrid series-parallel manipulation system, part-I: Position kinematics." *Proceedings from Winter Annual Meeting, American Society of Mechanical Engineers*. 1987.
Wang, C.C., and Y.Q. Zhu. "Identification and Machine Learning Prediction of Nonlinear Behavior in a Robotic Arm System." *Symmetry* 13.8 (2021): 1445.
Wang, Y.C., et al. "High performance both in low-speed tracking and large-angle swing scanning based on adaptive nonsingular fast terminal sliding mode control for a three-axis universal inertially stabilized platform." *Sensors* 20.20 (2020): 5785.
Xu, P, et al. "Kinematics analysis of a hybrid manipulator for computer-controlled ultra-precision freeform polishing." *Robotics and Computer-Integrated Manufacturing* 44 (2017): 44-56.
Ya, T, J L Du, and J Li. "PTESO based robust stabilization control and its application to 3-DOF ship-borne parallel platform." *Ocean Engineering* 284 (2023): 115202.
Yang, X, et al. "Dynamics and isotropic control of parallel mechanisms for vibration isolation." *IEEE/ASME Transactions on Mechatronics* 25.4 (2020): 2027-2034.
Yuan, X.M., et al. "Analysis of Vibration Characteristics of Electro-hydraulic Driven 3-UPS/S Parallel Stabilization Platform." *Chinese Journal of Mechanical Engineering* 37.1 (2024): 96.
Zhao, T.S., et al. "Stiffness and singularity analysis of foldable parallel mechanism for ship-based stabilized platform." *Robotica* 34.4 (2016): 913-924.
Zhao, X.Y., et al. "Kinematic analysis and dimensional synthesis of a three-degrees-of-freedom hybrid-drive parallel mechanism." *Proceedings of the Institution of Mechanical ·Engineers, Part C: Journal of Mechanical Engineering Science* 233.8 (2019): 2728-2752.
Zhang, M.Y., Yongliang Guan, and Weiwei Zhao. "Adaptive super-twisting sliding mode control for stabilization platform of laser seeker based on extended state observer." *Optik* 199 (2019): 163337.
Zhang, Z, et al. "Asymptotic stabilization control of fractional-order memristor-based neural networks system via combining vector Lyapunov function with M-matrix." *IEEE Transactions on Systems, Man, and Cybernetics: Systems* 53.3 (2022): 1734-1747.
Zhang, Z, et al. "Novel stability results of multivariable fractional-order system with time delay." *Chaos, Solitons & Fractals* 157 (2022): 111943.

串並聯船載穩定平臺的動態特性研究

曾天　張海峯　範狄慶　劉新田
上海工程技術大學機械與汽車工程學院

童博
西安熱工研究院有限公司

摘 要

針對傳統船載穩定平臺結構複雜、成本高、穩定性弱的問題，本文提出了一種串並聯船載穩定平臺，該平臺由串聯機構和並聯機構複合組成，具有結構簡單、穩定性好、控制精度高等優點。本文對該平臺的魯棒性進行了分析，並基於艦船的四種工作狀態進行了控制精度和動態特性實驗。結果表明，該平臺能夠有效抑制艦船的搖擺，具有良好的動態特性和控制精度，能夠滿足小型化、低成本和高性能的船載穩定平臺應用需求。